miR-10b-3p, miR-8112 and let-7j as potential biomarkers for autoimmune inner ear diseases

JUHONG ZHANG[1,2], NA WANG[2] and ANTING XU[2,3]

[1]Department of Otolaryngology, Shanghai Jiao Tong University Affiliated Sixth People's Hospital South Campus, Shanghai 201499; [2]Department of Otolaryngology/Head and Neck Surgery, The Second Hospital of Shandong University, Jinan, Shandong 250033; [3]Department of Otolaryngology, Affiliated Tenth People's Hospital of Tongji University, Shanghai 200072, P.R. China

Received April 10, 2018; Accepted March 15, 2019

DOI: 10.3892/mmr.2019.10248

Abstract. Circulating microRNAs (miRNAs) have been suggested as non-invasive biomarkers for the diagnosis of several autoimmune diseases. However, to the best of our knowledge, no studies have yet examined the miRNA expression profiles in autoimmune inner ear disease (AIED). The present study aimed to use an miRNA sequencing assay to detect the miRNA expression profiles of serum samples from 3 control mice and 3 antigen-induced AIED model mice. Differentially expressed miRNAs (DE-miRNAs) were screened using a t-test. miRNA target prediction was performed using TargetScan Mouse. Then, the miRNA-target gene interaction network was constructed and visualized using Cytoscape software. The underlying functions of the target genes of the DE-miRNAs were predicted using the clusterProfiler package. As a result, 22 miRNAs were identified as DE-miRNAs between AIED and control mice, including 10 upregulated and 12 downregulated genes. Based on the TargetScan Mouse prediction, 1,958 genes were identified as the targets for the 22 DE-miRNAs. Functional analysis indicated that only the target genes of 8 miRNAs were respectively enriched for Gene Ontology terms and Kyoto Encyclopedia of Genes and Genomes pathways, among which miR-10b-3p, let-7j and miR-8112 were shared between the two pathway analyses. These 3 miRNAs may be involved in AIED by affecting inflammatory chemokine (miR-10b-3p-C-C motif chemokine 12), Wnt signaling (miR-8112-Wnt9b/Wnt 3a/Wnt2b) and Mucin type O-glycan biosynthesis pathways (let-7j-Galnt2/Galnt12). In conclusion, miR-10b-3p, miR-8112 and let-7j may be underlying biomarkers for diagnosing AIED.

Correspondence to: Dr Anting Xu, Department of Otolaryngology/Head and Neck Surgery, The Second Hospital of Shandong University, 247 Beiyuan Street, Tianqiao, Jinan, Shandong 250033, P.R. China
E-mail: xueanting1709@tom.com

Key words: hearing loss, autoimmune diseases, inflammation, microRNAs

Introduction

Autoimmune inner ear disease (AIED) is a rare, but rapidly progressive, bilateral form of sensorineural hearing loss (SNHL) (1). Patients with AIED exhibit a loss of hearing over a period of weeks to months, often accompanied by tinnitus and vertigo, which may cause depressive thoughts and emotions, and disruption to daily activities and personal relationships for patients, ultimately affecting their quality of life (2,3). However, this disease is reversible, and early diagnosis of AIED with timely administration of glucocorticoids may prevent damage to the inner ear structures and result in hearing preservation. Therefore, the investigation of rapid and reliable diagnostic biomarkers for AIED is an important field of clinical study.

Although the pathogenesis of AIED remains unclear, accumulating evidence suggests that activation of the innate immune system may be the primary contributor (4). When an antigen enters the inner ear, it may be initially processed by the immunocompetent cells present in and around the endolymphatic sac. Through the secretion of various cytokines, these immunocompetent cells additionally stimulate migration of the inflammatory cells in the systemic circulation to the inner ear, subsequently amplifying the immune response and inducing more severe inner ear injuries (4-6). Therefore, several inflammatory cytokines, including tumor necrosis factor-α (TNF-α) (7), interleukin-1β (IL-1β), Il-6, IL-17 (8), C-X-C motif chemokine 10 (CXCL10) (9) and interferon-γ (IFN-γ) (10) have been suggested as biomarkers for the diagnosis of AIED. However, the implications of these biomarkers in a clinical setting remains limited and additional exploration of the key genes involved in the development of AIED is essential.

MicroRNAs (miRNAs) are endogenous, noncoding RNAs that have been demonstrated to serve an important role in regulating autoimmunity via binding to the 3'-untranslated region of their mRNA targets and thereby affecting the development of a number of autoimmune diseases (11). For example, Ishida *et al* (12) identified that the levels of miR-142-5p and miR-21 were significantly increased, whereas the level of miR-182 was significantly decreased, in experimental autoimmune uveoretinitis, and suggested that these miRNAs may

participate in immunity by affecting the expression of IL-17. Fang *et al* (13) demonstrated that the increased expression of miR-30a was associated with the development and progression of autoimmune encephalomyelitis. miR-30a increased the expression of pro-inflammatory IL-1β and inducible nitric oxide synthase in primary cultured mouse microglia. These data suggested that cytokine production and associated AIED may also be controlled by miRNAs. This hypothesis has been preliminarily supported by Rudnicki *et al* (14) who demonstrated that inflammatory stimuli in the inner ear induced activation of the innate immune system via miR-224 and its target pentraxin 3. Furthermore, Xin *et al* (15) also identified that compared with Fas(lpr/lpr) mice, a spontaneous AIED model accompanied by systemic lupus erythematosus, miR-155(-/-)Fas(lpr/lpr) mice exhibited decreased levels of total immunoglobulin (Ig)A, IgM and IgG and less infiltration of inflammatory cells in the kidney. In addition, the serum levels of IL-4 and IL-17a, secreted by T helper (Th)2 and Th17 cells, were decreased, and the cluster of differentiation (CD)4(+)/CD8(+) T cell ratio was restored in the miR-155(-/-) Fas(lpr/lpr) mice. These data implied that miR-155 may also be an important miRNA in the regulation of inflammation in AIED. However, the specific miRNAs that are involved in the development of AIED remain unclear. Therefore, the aim of the present study was to screen crucial serum miRNAs in an antigen-induced AIED mouse model.

Materials and methods

Experimental animals. A total of 10 male adult (4 weeks) white guinea pigs weighing ~270 g and 54 female C57BL/6 4-week old mice weighing ~15 g (specific pathogen-free) were purchased from the Shanghai Laboratory Animal Center. Animals were housed in a temperature- (20-25˚C) and humidity-controlled environment (40-70%). The animal procedures were performed in accordance with the Guide for the Care and Use of Laboratory Animals (16) and were approved by the Institutional Animal Care and Use Committees of Shandong University (Jinan, China).

Preparation of purified inner ear antigen. Following ether anesthesia, which was verified by the observation of muscle relaxation and loss of the pedal reflex with the presence of a normal heartbeat, guinea pigs were sacrificed by cardiac perfusion using cold PBS followed by cold 4% paraformaldehyde (17). Animal death was defined as mydriasis and respiratory arrest. The temporal bones were obtained following decapitation, which were then placed in 10 mM sterile TBS supplemented with 1 μg/ml aprotinin to isolate the inner ear tissue. Following homogenization and centrifugation at 100,000 x g for 1 h at 4˚C, the supernatant was separated and inner ear tissue antigen was prepared. The protein content was indirectly estimated by using a UV-Vis spectrophotometer at excitation and emission wavelengths of 260 and 280 nm, respectively (protein concentration =1.45 A280-0.74 A260) following sedimentation in TBS supplemented with 0.5% SDS, 0.5% mercaptoethanol, 1% glycerinum, 2 mM phenylmethylsulfonyl fluoride and 10 mM decyl maleic dimethylamine and centrifugation at 1,000 x g for 10 min at 4˚C.

Construction of an AIED animal model. The C57BL/6 mice were randomly assigned into three groups, including the control (n=18), immunization for 1 week (AIED-1; n=18) and immunization for 2 weeks (AIED-2; n=18) groups. Inner ear tissue antigen was emulsified with an equal volume of complete Freund's adjuvant (Sigma-Aldrich; Merck KGaA), which was subcutaneously injected (200 μl, containing 100 μg antigen) into multiple points in the neck and back of animals to induce AIED. In the control group, only complete Freund's adjuvant was injected. Injection sites were examined daily and reactogenicity was observed macroscopically (18). Pain was evaluated by torsion observation and topical opioids (19) were applied on the skin area if pain was present. All ulceration was observed macroscopically, and was spontaneously resolved without the requirement for treatment. The AIED model was confirmed by histopathological analysis of the cochlea via standard hematoxylin and eosin (H&E) staining: The cochlea tissue was fixed in 4% paraformaldehyde at 4˚C for 3-5 days, dehydrated in graded ethanol (80, 90, 95, 100% ethanol I, 100% ethanol II and 100% ethanol III, 5 min each, at room temperature), cleared in xylene (I, II, each 30 min, at room temperature), embedded in paraffin (I, 1 h; II, 6 h; at 65˚C) and sectioned to a thickness of 4 μm. Following deparaffinization and rehydration (xylene I 15 min, xylene II 15 min, 100% ethanol 5 min, 100% ethanol II 5 min, 95% ethanol 5 min, 80% ethanol 5 min, running water 1 min, at room temperature), the sections were stained with 0.5% hematoxylin and eosin for 5 min each at room temperature and then washed with distilled water. The slices were viewed under a light microscope (Olympus BX43; Olympus Corporation; magnification, x200).

Small RNAseq library preparation and sequencing. The serum samples of 3 AIED-1 and 3 control mice were obtained and subjected to miRNA deep sequencing analysis (LC Sciences). Briefly, total RNA was extracted from serum using TRIzol (Thermo Fisher Scientific, Inc.) and ligated to 3' and RNA 5' adapters of RNA at 70˚C for 2 min each. The total RNA was reverse transcribed into cDNA using the SuperrScript II Reverse Transcriptase (Invitrogen; Thermo Fisher Scientific, Inc.) at 50˚C for 1 h. PCR amplification was run with 25 μl reaction mixture, including 11.5 μl cDNA, 12.5 μl Phusion® Hot Start Flex 2X Master Mix (New England Biolabs, Inc.) and 0.5 μl primers (each, 5'-GATCGGAAGAGCACACGTCT GAACTCCAGTCACAAGACGGAATCTCGTATGCCGTC TTCTGCTTG-3'; 5'-AGATCGGAAGAGCGTCGTGTAGGG AAAGA-3'). PCR amplification was carried out under conditions of 98˚C for 3 sec followed by 12 cycles of 98˚C for 10 sec, 60˚C for 30 sec, and 72˚C for 15 sec, and 72˚C for 10 min. Small cDNA fractions were isolated by using 6% Tris-borate-EDTA/polyacrylamide gel electrophoresis (TBE-PAGE). Subsequently, the cDNA constructs were purified and the library was validated. Finally, the purified PCR products were used for sequencing analysis via the Illumina Solexa Sequencer (Illumina, Inc.). Raw sequencing reads were obtained using Illumina's Sequencing Control Studio software (v2.8; Illumina, Inc.).

Data preprocessing. Preliminary quality control analysis of the FASTQ files was performed with FASTQC software (v0.10.0; http://www.bioinformatics.babraham.ac.uk/

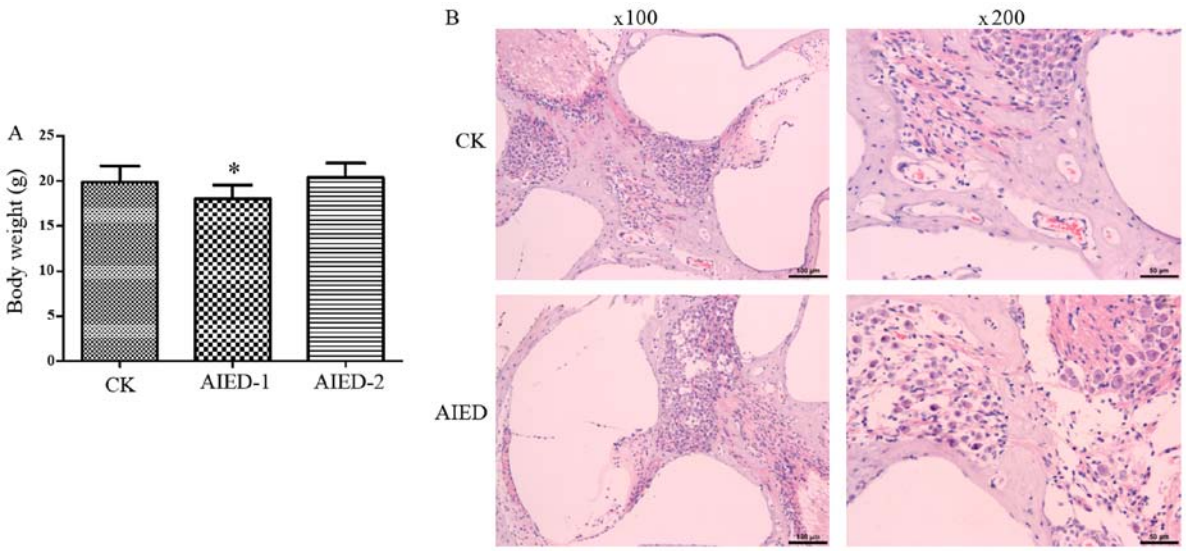

Figure 1. Construction of autoimmune inner ear disease model mice. (A) Measurement of body weight in each group. (B) Histopathological analysis of the cochlea via standard hematoxylin and eosin staining. 2, for two weeks. *P<0.05 vs. CK group. CK, control; AIED, autoimmune inner ear disease; AIED-1, 1 week AIED model; AIED-2, 2 week AIED model.

projects/fastqc/). Cutadapt (v1.1) (20) was then used to trim 5' (TGGAATTCTCGGGTGCCAAGG) and 3' (GTTCAGAGTTCTACAGTCCGACG) adaptor sequences. Reads that were <17 nucleotides following trimming were discarded. Trimmed reads were then additionally filtered using the FASTQC software.

Quantification of miRNA gene expression. miRDeep software (v 2.0) (21) was used to perform the qualitative and quantitative analysis for miRNAs. Briefly, the filtered 'clean reads' were aligned to mouse genome reference sequence (University of California Santa Cruz mm10) (22) using the Mapper module in miRDeep2 software, which uses the bowtie algorithm. Then, the Quantifier module from the miRDeep2 package was used to generate miRNAs alignment files against known miRNAs from an miRNA database (miRBASE release 20) (23). The novel miRNAs were predicted by the ViennaRNA (https://www.tbi.univie.ac.at/RNA/) (24) and RNAFold (25) algorithms from miRDeep2 package. The principal-component analysis (PCA) was performed using the 'Factoextra' package in R (v1.0.3) (26) to examine the associations and variation between samples.

Identification of differentially expressed miRNAs (DE-miRNAs). The quantitative miRNAs data were normalized to read per million (RPM), which was calculated as RPM = miRNA counts / total counts of each sample x 1,000,000, and then log 2-transformed. The DE-miRNAs between the control and AIED groups were identified using a paired Student's t-test. miRNAs were considered to be differentially expressed at P<0.05, fold change (FC) >1.5 or <1/1.5 and average expression >(log_2) 5 RPM. To determine whether the DE-miRNAs were able to differentiate AIED from control mice, clustering analysis (27) was performed to generate a heat map using the hclust function implemented in the R package (v2.14.1; http://www.R-project.org), which uses the Euclidean distance and Ward's method.

Target genes prediction of DE-miRNAs. miRNA target prediction was performed using the online software TargetScan Mouse (v7.1) (28). The threshold value was set at Context Score <-0.4. Then, the miRNA-target gene interaction network was constructed and visualized using Cytoscape software (v3.4; www.cytoscape.org/) (29).

Functional enrichment analysis. To examine the underlying functions of target genes of DE-miRNAs, Gene Ontology (GO) terms and Kyoto Encyclopedia of Genes and Genomes (KEGG) pathway enrichment analyses were performed using the clusterProfiler package in R (v3.0.1) (30) with the mouse annotations from package org.Mm.eg.db (v3.3.0) (31) and KEGG.db (v2.2.11) (32). P<0.05 and multiple-adjusted P<0.05 were set as the cut-off values.

Statistical analysis. The data are expressed as mean ± standard deviation, and were analyzed by GraphPad Prism software (v6; GraphPad Software, Inc.). The DE-miRNAs between the control and AIED groups were identified using a paired Student's t-test. Comparisons between multiple groups were performed by one-way analysis of variance followed by Duncan's post-hoc test. P<0.05 was considered to indicate a statistically significant difference.

Results

AIED model construction. In the control group, the hair of mice was smooth and glossy, and their body weight increased over time. However, in the inner ear tissue antigen immunization group, the activity of mice was decreased, with significantly decreased body weight after 1 week (Fig. 1A). In addition, slight ulceration, but no evidence of pain, was evident in the skin injected with the antigen. However, the ulcer scar was formed and then sloughed after 2 weeks, leading to a restored increase in the body weight in the AIED-2 group (Fig. 1A). These data suggest that the immune response was marked

Table I. Quality control and alignment results.

Sample	Raw reads	Following QC reads	Mapped reads	Mapped reads. %
Case 1	8,827,017	3,060,225	2,070,930	67.7
Case 2	12,375,221	9,365,942	6,493,558	69.3
Case 3	11,975,356	8,136,614	5,522,291	67.9
Ctrl 1	12,655,012	8,128,777	6,558,442	80.7
Ctrl 2	17,988,328	13,477,582	10,106,224	75.0
Ctrl 3	10,252,143	6,396,838	4,773,578	74.6

QC, quality control; Ctrl, control.

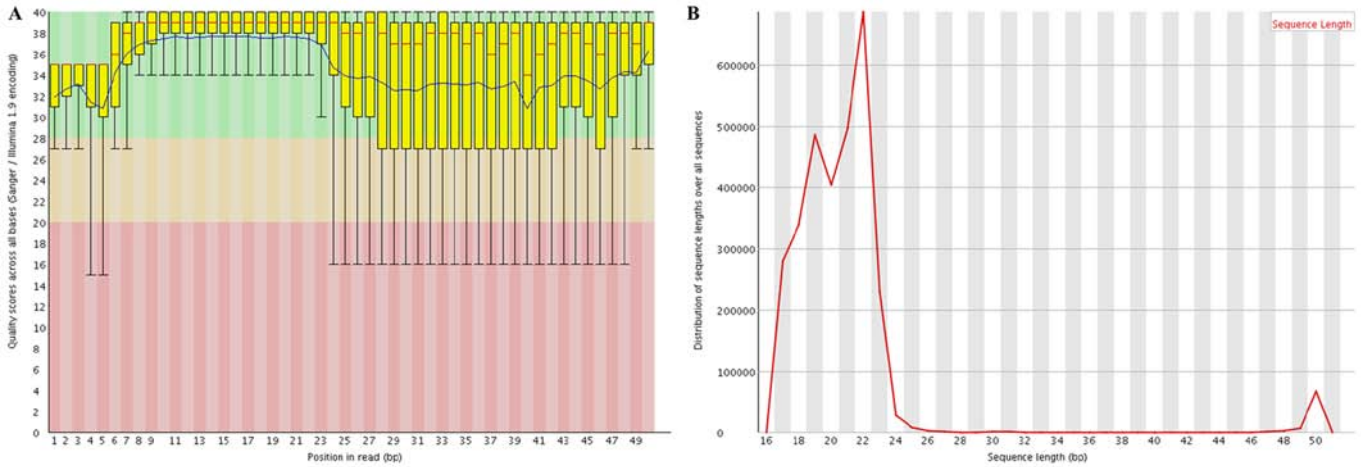

Figure 2. Quality control analysis. (A) Quality scores. (B) Length distribution. Bp, base pairs.

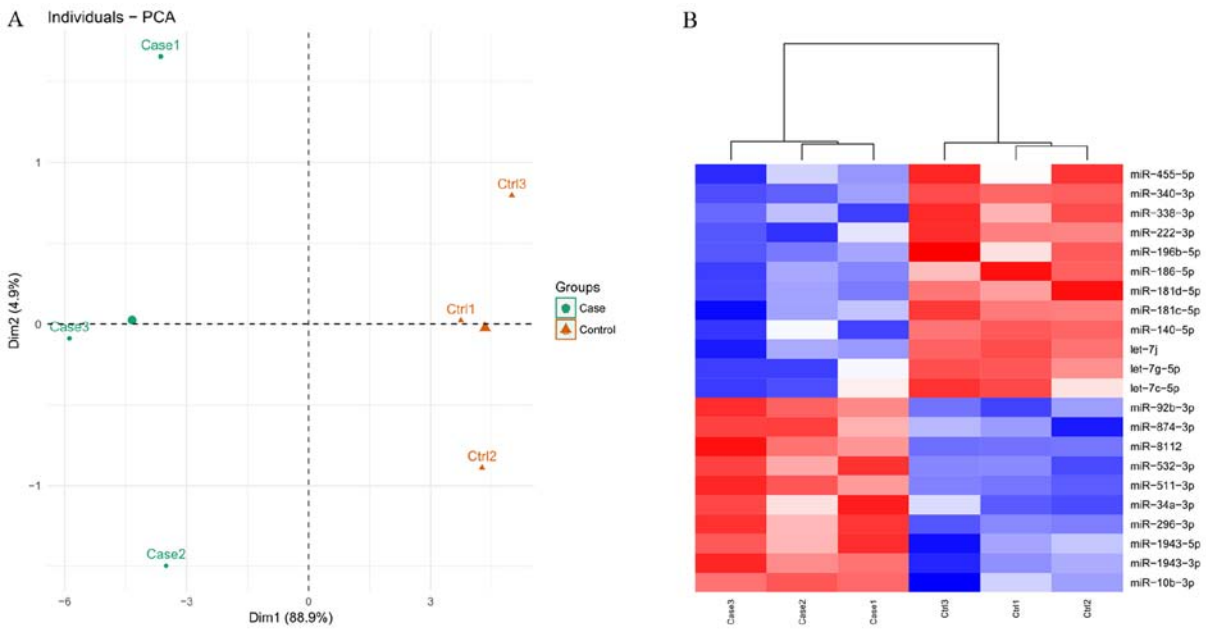

Figure 3. Cluster analysis. (A) Principal-component analysis for samples. (B) Heat map of differentially expressed miRNAs between autoimmune inner ear disease model mice and control groups. Red, upregulated; blue, downregulated. miR, microRNA, ctrl, control.

in the groups with inner ear tissue antigen immunization for 1 week and may have been sufficient to cause serious inner ears injuries. Subsequently, H&E staining was performed to observe the histopathological changes of the cochlea. As hypothesized, the inflammatory reactions in the inner ears of animals were evident in groups following immunization.

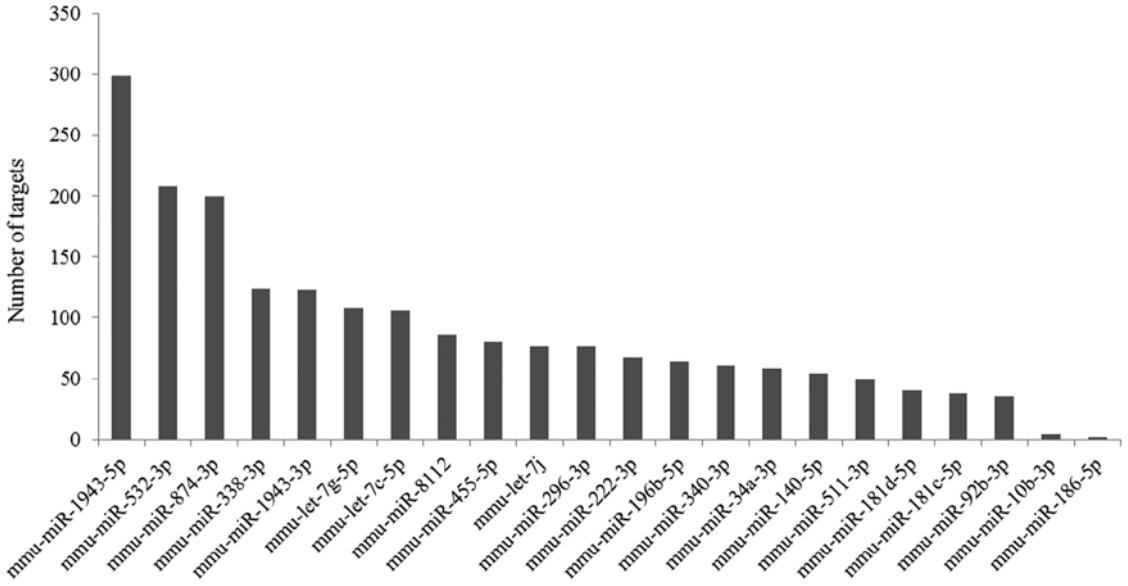

Figure 4. Number of target genes of differentially expressed miRNAs. miR, microRNA; mmu, *Mus musculus*.

Infiltration of inflammatory cells, primarily lymphocytes, was observed in the cochlear axis. The number of spiral ganglion cells was decreased and their distribution disordered. Shrinkage occurred in the organ of Corti, with a small level of necrosis observed in the outer hair cells. Vacuolar degeneration was occasionally visible in the hair cells of the cristae ampullaris (Fig. 1B). These changes were not present in the control mice, indicating that the AIED model was successfully established.

Identification of miRNAs. Following quality control analysis, 3,060,225-13,477,582 clean reads were obtained for the small RNA library. The length distribution analysis indicated that the majority of the reads were between 19-24 nucleotides (nt) long, with the most common length being 22 nt (Fig. 2). The trimmed reads were aligned against the mouse genome reference sequence. As a result, 67.7-80.7% of reads were mapped perfectly to the mouse genome (Table I), which were subsequently screened to identify known and novel miRNAs. Consequently, a total of 995 mature mouse miRNAs were identified and 337 novel miRNAs were annotated. PCA analysis (Fig. 3A) indicated that the known miRNAs clearly distinguished each AIED from each control sample, indicating there was there was a high level of consistency between samples.

Screening of DE-miRNAs and prediction of their target genes. A total of 22 miRNAs were identified as DE-miRNAs between AIED and control mice based on the thresholds, including 10 upregulated and 12 downregulated genes (Table II). The identified DE-miRNAs also significantly differentiated AIED from control samples according to the heat map presented in Fig. 3B.

Based on the TargetScan Mouse prediction, 1,958 genes were identified as the targets for the 22 DE-miRNAs. The number of target genes of each miRNA is demonstrated in Fig. 4. Then, a miRNA-mRNA interaction network was constructed, in which 1,696 genes and 22 miRNAs were included (Fig. 5).

Table II. Differentially expressed miRNAs screened.

miRNA	P-value	Fold change	Average expression (log_2 RPM)
mmu-let-7j	0.018	-0.42	9.73
mmu-miR-181c-5p	0.025	-0.45	8.12
mmu-miR-340-3p	0.003	-0.48	3.14
mmu-miR-181d-5p	0.007	-0.48	8.73
mmu-miR-186-5p	0.013	-0.50	9.04
mmu-miR-196b-5p	0.038	-0.55	6.05
mmu-miR-455-5p	0.042	-0.56	7.58
mmu-miR-338-3p	0.007	-0.60	6.42
mmu-let-7g-5p	0.034	-0.62	13.41
mmu-miR-140-5p	0.043	-0.62	9.82
mmu-let-7c-5p	0.045	-0.63	11.67
mmu-miR-222-3p	0.018	-0.65	11.19
mmu-miR-10b-3p	0.044	1.54	3.83
mmu-miR-34a-3p	0.024	1.57	2.56
mmu-miR-92b-3p	0.001	1.62	7.53
mmu-miR-1943-5p	0.020	1.71	4.11
mmu-miR-532-3p	0.005	1.74	6.53
mmu-miR-874-3p	0.011	1.76	4.74
mmu-miR-8112	0.017	1.82	6.14
mmu-miR-296-3p	0.014	2.17	5.59
mmu-miR-1943-3p	0.006	2.41	2.51
mmu-miR-511-3p	0.007	2.43	8.44

mmu, *Mus musculus*; miR, microRNA; RPM, read per million.

Functional enrichment analysis of target genes. Functional enrichment analysis was performed for all target genes to reveal their underlying functions. As a result, only the target genes of 8 miRNAs were enriched for GO terms (miR-10b-3p, let-7j,

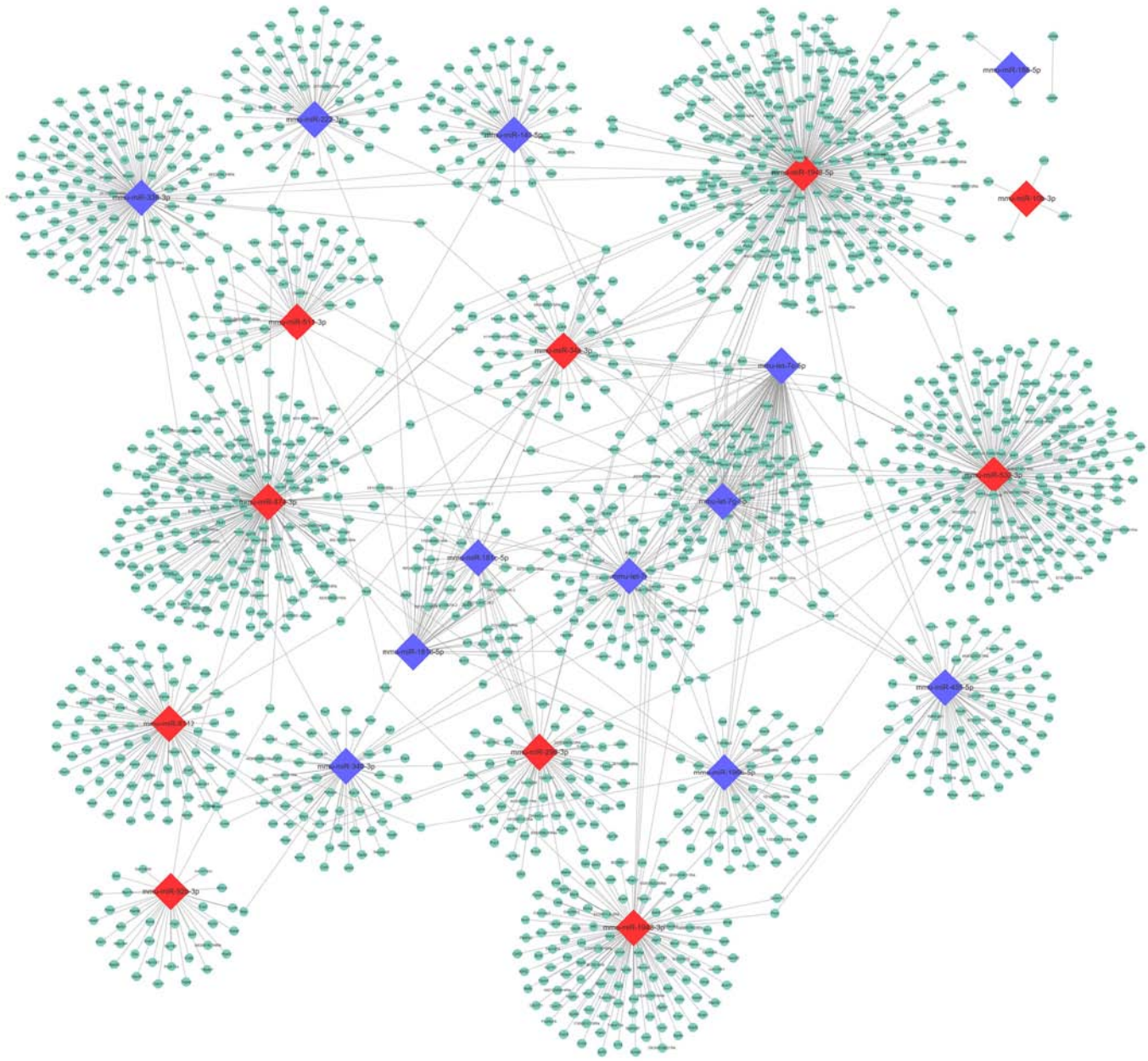

Figure 5. miRNA-mRNA interaction network. Diamond shapes represent miRNAs, and circles represent target genes. Red color denotes upregulated, and blue denotes downregulated. miR, microRNA.

miR-1943-5p, miR-196b-5p, miR-338-3p, miR-455-5p, miR-8112 and miR-92b-3p; Fig. 6) and KEGG pathways (miR-10b-3p, let-7c-5p, let-7g-5p, let-7j, miR-181c-5p, miR-181d-5p, miR-222-3p and miR-8112; Fig. 7), amongst which miR-10b-3p, let-7j and miR-8112 were common in each group. The results (Tables III and IV) indicated that miR-10b-3p may be particularly important for AIED as its target genes included inflammatory chemokines [including C-C motif chemokine (CCL) 12]. miR-8112 may be involved in AIED by affecting factors within the Wnt signaling pathway, including Wnt9b, Wnt 3a and Wnt2b (Tables III and IV). The target genes of let-7j were enriched in Glycosphingolipid biosynthesis - lacto and neolacto series and Mucin type O-glycan biosynthesis pathways, including polypeptide N-acetylgalactosaminyltransferase (Galnt) 2 and Galnt12 (Tables III and IV); these 2 pathways are associated with glycosylation, and induce the activation of the immune response.

Discussion

Previous studies have indicated that there are miRNA profiles associated with noise-induced hearing loss (33,34), but the AIED-associated miRNAs remain undetermined. To the best of our knowledge, the present study investigated, for the first time, the serum miRNA profiles in AIED by constructing an AIED mouse model. The results identified 22 DE-miRNAs in the AIED mice compared with the control mice. The functions of 13 of these miRNAs were enriched, among which miR-10b-3p, miR-8112 and let-7j may be particularly important for the development of AIED, as suggested by the GO and KEGG pathway enrichment analysis of their target genes, in which they were predicted to affect chemokine signaling (miR-10b-3p-Ccl12), Wnt signaling (miR-8112-Wnt9b; miR-8112-wnt 3a and miR-8112-Wnt2b) and O-glycan biosynthesis pathways (let-7j-Galnt2a and

Figure 6. Gene ontology enrichment terms for differentially expressed miRNAs. miR, microRNA.

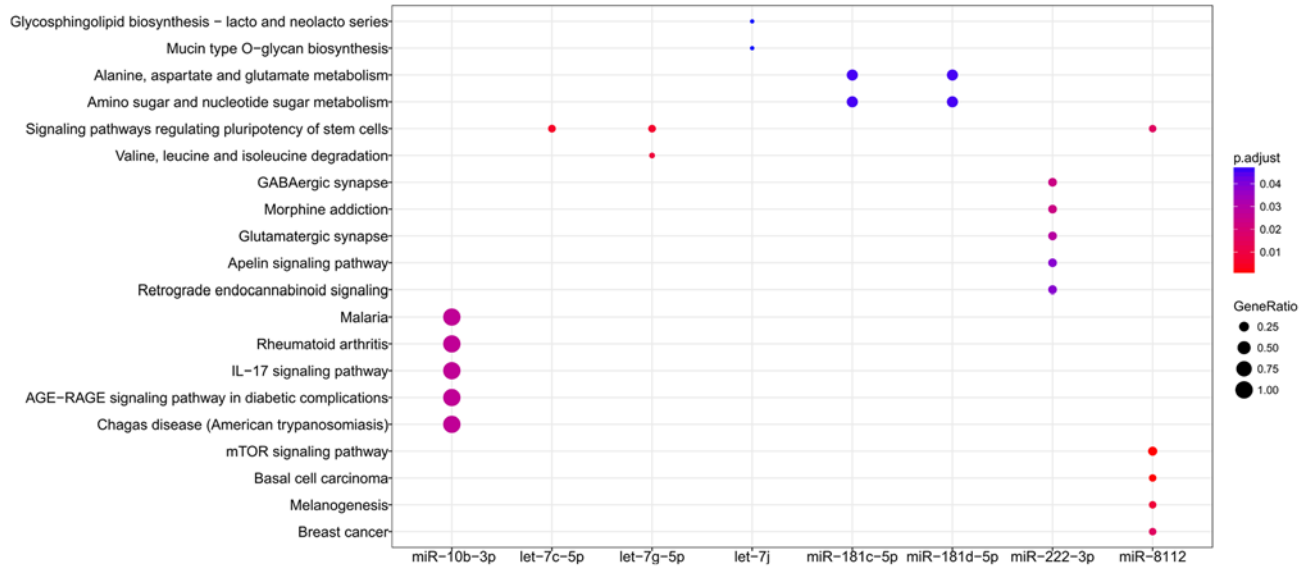

Figure 7. Kyoto Encyclopedia of Genes and Genomes pathway enrichment analyses for differentially expressed miRNAs. miR, microRNA.

let-7j-Galnt12). This appears to be in concordance with the previously identified inflammatory mechanisms of AIED (4).

It has been suggested that miR-10b was significantly upregulated in ankylosing spondylitis (35), which is a common autoimmune disease associated with the induction of SNHL (36-38). Therefore, miR-10b may also be hypothesized to be highly expressed in AIED, which was demonstrated in the present study (FC =1.54; P=0.04). However, Chen *et al* (35) identified that miR-10b overexpression inhibited the production of IL-17A by total CD4 and differentiating Th17 cells, suggesting that miR-10b may likely constitute part of a negative feedback loop that restricts the enhanced inflammatory Th17 responses. Although these results appeared to be inconsistent with our data, they may be reasonable as the present study similarly predicted that miR-10b may downregulate CCL12, a known inflammatory chemokine (39). Furthermore, it has been demonstrated that the use of the C-C chemokine receptor type 2 agonists, CCL2 and CCL12, elicited migration in Th17-polarized cells and additionally stimulated a modest enrichment of IL-17(+) cells (40). Therefore, miR-10b may serve crucial roles in AIED by regulating CCL-12 mediated Th17 responses. However, additional exploration of the roles of miR-10b-3p in AIED is required, as the study conducted by Mojsilovic-Petrovic *et al* (39) only examined the role of miR-10b-5p, although it may be inferred that miR-10b-3p may have a similar effect to miR-10b-5p (41).

miR-8112 is a rarely studied miRNA involved in disease, with the exception of one study by Wang *et al* (42), which indicated that miR-8112 was highly expressed in MC3T3-E1 cells exposed to high-dose fluoride and may induce the formation of impaired bone diseases, including skeletal fluorosis. Patients with skeletal fluorosis have also been demonstrated to exhibit varying degrees of hearing loss (43). Therefore, miR-8112 was hypothesized to be upregulated in AIED, which was verified in the results of the present study (FC=1.82; P=0.02). Notably, the present study suggested that inhibition of Wnt signaling pathway genes (Wnt9b, Wnt 3a and Wnt2b) may be an underlying mechanism of miR-8112, which has not been demonstrated previously,

Table III. GO enrichment for the target genes of differentially expressed miRNAs.

Cluster	ID	Description	P-value	Adjusted P-value	Gene ID
let-7j	GO:0016863	Intramolecular oxidoreductase activity, transposing C=C bonds	$1.07x10^{5}$	$2.99x10^{3}$	Hsd3b6, Hsd3b3, Hsd3b2
let-7j	GO:0008378	Galactosyltransferase activity	$1.20x10^{4}$	$7.81x10^{3}$	B3gnt5, Galnt2, Fut9, Galnt12
let-7j	GO:0008375	Acetylglucosaminyltransferase activity	$2.42x10^{4}$	$7.81x10^{3}$	B3gnt5, Galnt2, Fut9, Galnt12
let-7j	GO:0033764	Steroid dehydrogenase activity, acting on the CH-OH group of donors, NAD or NADP as acceptor	$3.63x10^{4}$	$7.81x10^{3}$	Hsd3b6, Hsd3b3, Hsd3b2
let-7j	GO:0016229	Steroid dehydrogenase activity	$4.99x10^{4}$	$7.81x10^{3}$	Hsd3b6, Hsd3b3, Hsd3b2
miR-196b-5p	GO:0000978	RNA polymerase II core promoter proximal region sequence-specific DNA binding	$2.53x10^{4}$	$2.42x10^{2}$	Nr6a1, Hoxa7, Otx1, Hoxa5, Hand1, Sarnp
miR-196b-5p	GO:0000987	Core promoter proximal region sequence-specific DNA binding	$3.44x10^{4}$	$2.42x10^{2}$	Nr6a1, Hoxa7, Otx1, Hoxa5, Hand1, Sarnp
miR-196b-5p	GO:0001159	Core promoter proximal region DNA binding	$3.60x10^{4}$	$2.42x10^{2}$	Nr6a1, Hoxa7, Otx1, Hoxa5, Hand1, Sarnp
miR-196b-5p	GO:0000982	Transcription factor activity, RNA polymerase II core promoter proximal region sequence-specific binding	$3.76x10^{4}$	$2.42x10^{2}$	Nr6a1, Hoxa7, Otx1, Hoxa5, Hand1, Sarnp
miR-196b-5p	GO:0008201	Heparin binding	$5.62x10^{4}$	$2.90x10^{2}$	Fgfbp3, Lxn, Prss57, Ecm2
miR-455-5p	GO:0008766	UDP-N-acetylmuramoylalanyl-D-glutamyl-2, 6-diaminopimelate-D-alanyl-D-alanine ligase activity	$9.11x10^{4}$	$2.14x10^{2}$	Nr6a1, Hoxa7, Otx1, Hoxa5, Hand1, Sarnp
miR-455-5p	GO:0018169	Ribosomal S6-glutamic acid ligase activity	$9.11x10^{4}$	$2.14x10^{2}$	Nr6a1, Hoxa7, Otx1, Hoxa5, Hand1, Sarnp
miR-455-5p	GO:0043773	Coenzyme F420-0 gamma-glutamyl ligase activity	$9.11x10^{4}$	$2.14x10^{2}$	Nr6a1, Hoxa7, Otx1, Hoxa5, Hand1, Sarnp
miR-455-5p	GO:0043774	Coenzyme F420-2 alpha-glutamyl ligase activity	$9.11x10^{4}$	$2.14x10^{2}$	Nr6a1, Hoxa7, Otx1, Hoxa5, Hand1, Sarnp
miR-455-5p	GO:0070735	Protein-glycine ligase activity	$9.11x10^{4}$	$2.14x10^{2}$	Fgfbp3, Lxn, Prss57, Ecm2
miR-338-3p	GO:0005096	GTPase activator activity	$1.76x10^{4}$	$1.76x10^{4}$	Nr6a1, Hoxa7, Otx1, Hoxa5, Hand1, Sarnp
miR-338-3p	GO:0030695	GTPase regulator activity	$2.94x10^{4}$	$2.94x10^{4}$	Nr6a1, Hoxa7, Otx1, Hoxa5, Hand1, Sarnp
miR-338-3p	GO:0005088	Ras guanyl-nucleotide exchange factor activity	$3.44x10^{4}$	$3.44x10^{4}$	Nr6a1, Hoxa7, Otx1, Hoxa5, Hand1, Sarnp
miR-338-3p	GO:0005089	Rho guanyl-nucleotide exchange factor activity	$4.38x10^{4}$	$4.38x10^{4}$	Nr6a1, Hoxa7, Otx1, Hoxa5, Hand1, Sarnp
miR-338-3p	GO:0051082	Unfolded protein binding	$4.88x10^{4}$	$4.88x10^{4}$	Fgfbp3, Lxn, Prss57, Ecm2
miR-10b-3p	GO:0001106	RNA polymerase II transcription corepressor activity	$4.20x10^{3}$	$3.67x10^{3}$	76365
miR-10b-3p	GO:0043175	RNA polymerase core enzyme binding	$4.20x10^{3}$	$4.20x10^{3}$	Rprd1b
miR-10b-3p	GO:0048020	CCR chemokine receptor binding	$5.59x10^{3}$	$5.59x10^{3}$	Ccl12
miR-10b-3p	GO:0008009	Chemokine activity	$6.81x10^{3}$	$6.81x10^{3}$	Ccl12
miR-10b-3p	GO:0042379	Chemokine receptor binding	$8.73x10^{3}$	$8.73x10^{3}$	Ccl12
miR-92b-3p	GO:0008198	Ferrous iron binding	$5.34x10^{4}$	$5.34x10^{4}$	Isca1, 432732
miR-92b-3p	GO:0051537	2 iron, 2 sulfur cluster binding	$6.84x10^{4}$	$6.84x10^{4}$	Isca1, 432732
miR-92b-3p	GO:0004364	Glutathione transferase activity	$9.74x10^{4}$	$9.74x10^{4}$	Gsta2, Gm10639
miR-92b-3p	GO:0051539	4 iron, 4 sulfur cluster binding	$1.62x10^{3}$	$1.62x10^{3}$	Isca1, 432732
miR-1943-5p	GO:0030374	Ligand-dependent nuclear receptor transcription coactivator activity	$1.57x10^{5}$	$1.57x10^{5}$	Atxn7l3, Usp22, 15361, Actn2; Hmga1-rs1, Rbm14
miR-8112	GO:0005109	Frizzled binding	$1.14x10^{5}$	$1.14x10^{5}$	Ror2, Wnt9b, Wnt3a, Wnt2b

GO, Gene ontology.

Table IV. Kyoto Encyclopedia of Genes and Genomes pathway enrichment for the target genes of differentially expressed miRNAs..

Cluster	ID	Description	P-value	Adjusted P-value	Gene ID
let-7j	mmu00601	Glycosphingolipid biosynthesis - lacto and neolacto series	$2.85x10^{3}$	$4.75x10^{2}$	B3gnt5, Fut9
let-7j	mmu00512	Mucin type O-glycan biosynthesis	$3.06x10^{3}$	$4.75x10^{2}$	Galnt2, Galnt12
miR-181c-5p	mmu00250	Alanine, aspartate and glutamate metabolism	$1.37x10^{2}$	$4.53x10^{2}$	Gfpt1
miR-181c-5p	mmu00520	Amino sugar and nucleotide sugar metabolism	$1.81x10^{2}$	$4.53x10^{2}$	Gfpt1
miR-181d-5p	mmu00250	Alanine, aspartate and glutamate metabolism	$1.37x10^{2}$	$4.53x10^{2}$	Gfpt1
miR-181d-5p	mmu00520	Amino sugar and nucleotide sugar metabolism	$1.81x10^{2}$	$4.53x10^{2}$	Gfpt1
let-7g-5p	mmu04550	Signaling pathways regulating pluripotency of stem cells	$6.84x10^{5}$	$6.57x10^{3}$	Smarcad1, Skil, Wnt16, Hand1, Hoxb1, Acvr1c
let-7g-5p	mmu00280	Valine, leucine and isoleucine degradation	$1.92x10^{4}$	$9.22x10^{3}$	Agxt2, Bcat1, Ehhadh, Acat1
let-7c-5p	mmu04550	Signaling pathways regulating pluripotency of stem cells	$5.95x10^{5}$	$5.59x10^{3}$	Smarcad1, Skil, Wnt16, Hand1, Hoxb1, Acvr1c
miR-222-3p	mmu04727	GABAergic synapse	$6.35x10^{4}$	$2.35x10^{2}$	Gng5, Gabra1, Gnb3
miR-222-3p	mmu05032	Morphine addiction	$7.23x10^{4}$	$2.35x10^{2}$	Gng5, Gabra1, Gnb3
miR-222-3p	mmu04724	Glutamatergic synapse	$1.35x10^{3}$	$2.92x10^{2}$	Gng5, Ppp3r1, Gnb3
miR-222-3p	mmu04371	Apelin signaling pathway	$2.38x10^{3}$	$3.85x10^{2}$	Agtr1a, Gng5, Gnb3
miR-222-3p	mmu04723	Retrograde endocannabinoid signaling	$2.96x10^{3}$	$3.85x10^{2}$	Gng5, Gabra1, Gnb3
miR-222-3p	mmu04151	PI3K-Akt signaling pathway	$4.02x10^{3}$	$4.36x10^{2}$	Ddit4, Gng5, Gnb3, Kit
miR-10b-3p	mmu05144	Malaria	$6.08x10^{3}$	$2.68x10^{2}$	Ccl12
miR-10b-3p	mmu05323	Rheumatoid arthritis	$1.03x10^{2}$	$2.68x10^{2}$	Ccl12
miR-10b-3p	mmu04657	IL-17 signaling pathway	1.13x102	$2.68x102^{4}$	Ccl12
miR-10b-3p	mmu04933	AGE-RAGE signaling pathway in diabetic complications	$1.24x10^{2}$	$2.68x10^{2}$	Ccl12
miR-10b-3p	mmu05142	Chagas disease (American trypanosomiasis)	$1.26x10^{2}$	$2.68x10^{2}$	Ccl12
miR-10b-3p	mmu04668	TNF signaling pathway	$1.34x10^{2}$	$2.68x10^{2}$	Ccl12
miR-10b-3p	mmu05418	Fluid shear stress and atherosclerosis	$1.76x10^{2}$	$2.78x10^{2}$	Ccl12
miR-10b-3p	mmu04621	NOD-like receptor signaling pathway	$2.08x10^{2}$	$2.78x10^{2}$	Ccl12
miR-10b-3p	mmu05164	Influenza A	$2.08x10^{2}$	$2.78x10^{2}$	Ccl12
miR-10b-3p	mmu04062	Chemokine signaling pathway	$2.42x10^{2}$	$2.90x10^{2}$	Ccl12
miR-10b-3p	mmu05168	Herpes simplex infection	$2.67x10^{2}$	$2.91x10^{2}$	Ccl12
miR-10b-3p	mmu04060	Cytokine-cytokine receptor interaction	$3.36x10^{2}$	$3.36x10^{2}$	Ccl12
miR-8112	mmu04150	mTOR signaling pathway	$1.40x10^{2}$	$8.55x10^{4}$	Fzd8, Clip1, Wnt9b, Wnt3a, Wnt2b, Lpin1
miR-8112	mmu05217	Basal cell carcinoma	$4.06x10^{5}$	$1.24x10^{3}$	Fzd8, Wnt9b, Wnt3a, Wnt2b
miR-8112	mmu04916	Melanogenesis	$4.17x10^{4}$	$8.48x10^{3}$	Fzd8, Wnt9b, Wnt3a, Wnt2b
miR-8112	mmu04550	Signaling pathways regulating pluripotency of stem cells	$1.36x10^{3}$	$1.60x10^{2}$	Fzd8, Wnt9b, Wnt3a, Wnt2b
miR-8112	mmu05224	Breast cancer	$1.64x10^{3}$	$1.60x10^{2}$	Fzd8, Wnt9b, Wnt3a, Wnt2b
miR-8112	mmu04310	Wnt signaling pathway	$1.72x10^{3}$	$1.60x10^{2}$	Fzd8, Wnt9b, Wnt3a, Wnt2b
miR-8112	mmu04390	Hippo signaling pathway	$2.10x10^{3}$	$1.60x10^{2}$	Fzd8, Wnt9b, Wnt3a, Wnt2b
miR-8112	mmu00532	Glycosaminoglycan biosynthesis - chondroitin sulfate/dermatan sulfate	$2.28x10^{3}$	$1.60x10^{2}$	Chst15, B3galt6
miR-8112	mmu05200	Pathways in cancer	$2.36x10^{3}$	$1.60x10^{2}$	Fzd8, Wnt9b, Lpar1, Wnt3a, Wnt2b, Bcr
miR-8112	mmu04974	Protein digestion and absorption	$3.98x10^{3}$	$2.43x10^{2}$	Col2a1, Atp1a2, Col11a1
miR-8112	mmu05205	Proteoglycans in cancer	$5.96x10^{3}$	$3.30x10^{2}$	Fzd8; Wnt9b, Wnt3a, Wnt2b

miR, microRNA; mmu, *Mus musculus*.

to the best of our knowledge. This prediction may be indirectly supported by the observation that the loss of Wnt/β-catenin made hair cells more vulnerable to neomycin-induced injury and caused hearing loss (44), while activation of Wnt/β-catenin markedly promoted the mitotic regeneration of new hair cells and attenuated neurodegeneration in the auditory cortex (45,46). The association between the Wnt signaling pathway and AIED may also be associated with the inflammatory and oxidative stress, as the study by Liu *et al* (44) indicated that loss of β-catenin in hair cells led to decreased expression of antioxidant enzymes.

The Let-7 miRNA family has been suggested to exert inhibitory effects on the inflammation. For example, Brennan *et al* (47) observed that ectopic overexpression of let-7 inhibited the inflammatory responses including proliferation, migration, monocyte adhesion and NF-κB activation in vascular smooth muscle cells. In addition, Kumar *et al* (48) demonstrated that exogenous administration of let-7 mimics decreased IL-13 levels and relieved allergic airway inflammation. In concordance with these studies, the present study identified that let-7j, let-7g-5p and let-7c-5p were also downregulated in AIED mice. In addition, subsequent analysis also revealed that let-7j may be involved in AIED by regulating Galnts. Galnts are enzymes responsible for initiating the cascade of mucin-type O-linked glycosylation for certain inflammation-associated proteins, including selectin ligands. Block *et al* (49) demonstrated that compared with wild-type mice, L-selectin-dependent leukocyte rolling was completely abolished in Galnt1(-/-) mice, as its ligand was not able to be glycosylated by Galnt1. Although Galnt1 and Galnt12 have not been demonstrated in AIED, we hypothesized they may be upregulated by let-7j; however, this requires additional investigation.

In conclusion, the present study preliminarily revealed several important inflammatory-associated miRNAs, miR-10b-3p, miR-8112 and let-7j, in an AIED mouse model. They may be potential biomarkers and their abnormal expression may be conducive to early diagnosis of AIED and timely treatment with glucocorticoids. However, additional studies are required to confirm their diagnostic values using clinical samples and to investigate the direct interaction between these miRNAs and their target genes, including miR-10b-3p-Ccl12, miR-8112-Wnt9b/Wnt 3a/Wnt2b and let-7j-Galnt2/Galnt12.

Acknowledgements

Not applicable.

Funding

The present study was supported by National Natural Science Foundation of China (grant nos., 81371084 and 81570924).

Availability of data and materials

The datasets used and/or analyzed during the current study are available from the corresponding author on reasonable request.

Authors' contributions

JZ and AX participated in the design of this study. JZ and NW performed the animal model experiments. JZ performed the bioinformatics analyses. NW and AX contributed to the acquisition and interpretation of data. JZ was involved in drafting the manuscript. AX was involved in the manuscript revision. All authors read and approved the final manuscript.

Ethics approval and consent to participate

The animal procedures were approved by the Institutional Animal Care and Use Committees at Shandong University.

Patient consent for publication

Not applicable.

Competing interests

The authors declare that they have no competing interests.

References

1. Matsuoka AJ and Harris JP: Autoimmune inner ear disease: A retrospective review of forty-seven patients. Audiol Neurotol 18: 228-239, 2013.
2. Chen J, Liang J, Ou J and Cai W: Mental health in adults with sudden sensorineural hearing loss: An assessment of depressive symptoms and its correlates. J Psychosom Res 75: 72-74, 2013.
3. Carlsson PI, Hall M, Lind KJ and Danermark B: Quality of life, psychosocial consequences, and audiological rehabilitation after sudden sensorineural hearing loss. Int J Audiol 50: 139-144, 2011.
4. Goodall AF and Siddiq MA: Current understanding of the pathogenesis of autoimmune inner ear disease: A review. Clin Otolaryngol 40: 412-419, 2015.
5. Gopen Q, Keithley EM and Harris JP: Mechanisms underlying autoimmune inner ear disease. Drug Discov Today Dis Mech 3: 137-142, 2006.
6. Satoh H, Firestein GS, Billings PB, Harris JP and Keithley EM: Proinflammatory cytokine expression in the endolymphatic sac during inner ear inflammation. J Assoc Res Otolaryngol 4: 139-147, 2003.
7. Svrakic M, Pathak S, Goldofsky E, Hoffman R, Chandrasekhar SS, Sperling N, Alexiades G, Ashbach M and Vambutas A: Diagnostic and prognostic utility of measuring tumor necrosis factor in the peripheral circulation of patients with immune-mediated sensorineural hearing loss. Arch Otolaryngol Head Neck Surg 138: 1052-1058, 2012.
8. Pathak S, Hatam LJ, Bonagura V and Vambutas A: Innate immune recognition of molds and homology to the inner ear protein, cochlin, in patients with autoimmune inner ear disease. J Clin Immunol 33: 1204-1215, 2013.
9. Lee JM, Kim JY, Bok J, Kim KS, Choi JY and Kim SH: Identification of evidence for autoimmune pathology of bilateral sudden sensorineural hearing loss using proteomic analysis. Clin Immunol 183: 24-35, 2017.
10. Lorenz RR, Solares CA, Williams P, Sikora J, Pelfrey CM, Hughes GB and Tuohy VK: Interferon-γ production to inner ear antigens by T cells from patients with autoimmune sensorineural hearing loss. J Neuroimmunol 130: 173-178, 2002.
11. Chen JQ, Papp G, Szodoray P and Zeher M: The role of microRNAs in the pathogenesis of autoimmune diseases. Autoimmun Rev 15: 1171-1180, 2016.
12. Ishida W, Fukuda K, Higuchi T, Kajisako M, Sakamoto S and Fukushima A: Dynamic changes of microRNAs in the eye during the development of experimental autoimmune uveoretinitis. Invest Ophthalmol Vis Sci 52: 611-617, 2011.
13. Fang X, Sun D, Wang Z, Yu Z, Liu W, Pu Y, Wang D, Huang A, Liu M, Xiang Z, *et al*: miR-30a positively regulates the inflammatory response of microglia in experimental autoimmune encephalomyelitis. Neurosci Bull 33: 603-615, 2017.
14. Rudnicki A, Shivatzki S, Beyer LA, Takada Y, Raphael Y and Avraham KB: MicroRNA-224 regulates Pentraxin 3, a component of the humoral arm of innate immunity, in inner ear inflammation. Hum Mol Genet 23: 3138-3146, 2014.

15. Xin Q, Li J, Dang J, Bian X, Shan S, Yuan J, Qian Y, Liu Z, Liu G, Yuan Q, *et al*: miR-155 deficiency ameliorates autoimmune inflammation of systemic lupus erythematosus by targeting S1pr1 in Faslpr/lpr mice. J Immunol 194: 5437-5445, 2015.
16. National Research Council (US) Institute for Laboratory Animal Research: Guide for the Care and Use of Laboratory Animals. National Academies Press (US), Washingto, DC, 1996.
17. Watanabe K, Inai S, Jinnouchi K, Baba S and Yagi T: Expression of caspase-activated deoxyribonuclease (CAD) and caspase 3 (CPP32) in the cochlea of cisplatin (CDDP)-treated guinea pigs. Auris Nasus Larynx 30: 219-225, 2003.
18. Silva-Gomes R, Marcq E, Trigo G, Gonçalves CM, Longatto-Filho A, Castro AG, Pedrosa J and Fraga AG: Spontaneous healing of *Mycobacterium ulcerans* lesions in the guinea pig model. PLoS Negl Trop Dis 9: e0004265, 2015.
19. Poonawala T, Levay-Young BK, Hebbel RP and Gupta K: Opioids heal ischemic wounds in the rat. Wound Repair Regen 13: 165-174, 2005.
20. Martin M: Cutadapt removes adapter sequences from high-throughput sequencing reads. EMBnet J 17: 10-12, 2011.
21. Friedländer MR, Mackowiak SD, Li N, Chen W and Rajewsky N: miRDeep2 accurately identifies known and hundreds of novel microRNA genes in seven animal clades. Nucleic Acids Res 40: 37-52, 2012.
22. Haeussler M, Zweig AS, Tyner C, Speir ML, Rosenbloom KR, Raney BJ, Lee CM, Lee BT, Hinrichs AS, Gonzalez JN, *et al*: The UCSC Genome Browser database: 2019 update. Nucleic Acids Res 47 (D1): D853-D858, 2019.
23. Kozomara A and Griffiths-Jones S: miRBase: Annotating high confidence microRNAs using deep sequencing data. Nucleic Acids Res 42 (D1): D68-D73, 2014.
24. Lorenz R, Bernhart SH, Höner Zu Siederdissen C, Tafer H, Flamm C, Stadler PF and Hofacker IL: ViennaRNA Package 2.0. Algorithms Mol Biol 6: 26, 2011.
25. Bonnet E, Wuyts J, Rouzé P and Van de Peer Y: Evidence that microRNA precursors, unlike other non-coding RNAs, have lower folding free energies than random sequences. Bioinformatics 20: 2911-2917, 2004.
26. Kassambara A and Mundt F: factoextra: Extract and Visualize the Results of Multivariate Data Analyses. R package version 1.0.3, 2017. https://rpkgs.datanovia.com/factoextra/index.html.
27. Gu Z, Eils R and Schlesner M: Complex heatmaps reveal patterns and correlations in multidimensional genomic data. Bioinformatics 32: 2847-2849, 2016.
28. Agarwal V, Bell GW, Nam JW and Bartel DP: Predicting effective microRNA target sites in mammalian mRNAs. eLife 4: 4, 2015.
29. Shannon P, Markiel A, Ozier O, Baliga NS, Wang JT, Ramage D, Amin N, Schwikowski B and Ideker T: Cytoscape: A software environment for integrated models of biomolecular interaction networks. Genome Res 13: 2498-2504, 2003.
30. Yu G, Wang LG, Han Y and He QY: clusterProfiler: An R package for comparing biological themes among gene clusters. OMICS 16: 284-287, 2012.
31. Carlson M: org.Mm.eg.db: Genome wide annotation for Mouse. R package version 3.7.0, 2018. https://bioconductor.org/packages/release/data/annotation/html/org.Mm.eg.db.html.
32. Carlson M. KEGG.db: A set of annotation maps for KEGG. R package version 3.2.3, 2016. https://bioconductor.org/packages/release/data/annotation/html/KEGG.db.html.
33. Ding L, Liu J, Shen HX, Pan LP, Liu QD, Zhang HD, Han L, Shuai LG, Ding EM, Zhao QN, *et al*: Analysis of plasma microRNA expression profiles in male textile workers with noise-induced hearing loss. Hear Res 333: 275-282, 2016.
34. Li YH, Yang Y, Yan YT, Xu LW, Ma HY, Shao YX, Cao CJ, Wu X, Qi MJ, Wu YY, *et al*: Analysis of serum microRNA expression in male workers with occupational noise-induced hearing loss. Braz J Med Biol Res 51: e6426, 2018.
35. Chen L, Al-Mossawi MH, Ridley A, Sekine T, Hammitzsch A, de Wit J, Simone D, Shi H, Penkava F, Kurowska-Stolarska M, *et al*: miR-10b-5p is a novel Th17 regulator present in Th17 cells from ankylosing spondylitis. Ann Rheum Dis 76: 620-625, 2017.
36. Eryilmaz A, Dagli M, Karabulut H, Sivas Acar F, Erkol Inal E and Gocer C: Evaluation of hearing loss in patients with ankylosing spondylitis. J Laryngol Otol 121: 845-849, 2007.
37. Kahveci OK, Demirdal US, Duran A, Altuntas A, Kavuncu V and Okur E: Hearing and cochlear function of patients with ankylosing spondylitis. Clin Rheumatol 31: 1103-1108, 2012.
38. Sugahara K, Hashimoto M, Hirose Y, Shimogori H and Yamashita H: Autoimmune inner ear disease associated with ankylosing spondylitis. Egypt J Otolaryngol 30: 176-179, 2014.
39. Mojsilovic-Petrovic J, Callaghan D, Cui H, Dean C, Stanimirovic DB and Zhang W: Hypoxia-inducible factor-1 (HIF-1) is involved in the regulation of hypoxia-stimulated expression of monocyte chemoattractant protein-1 (MCP-1/CCL2) and MCP-5 (Ccl12) in astrocytes. J Neuroinflammation 4: 12, 2007.
40. Webb A, Johnson A, Fortunato M, Platt A, Crabbe T, Christie MI, Watt GF, Ward SG and Jopling LA: Evidence for PI-3K-dependent migration of Th17-polarized cells in response to CCR2 and CCR6 agonists. J Leukoc Biol 84: 1202-1212, 2008.
41. Yoon EL, Yeon JE, Ko E, Lee HJ, Je JH, Yoo YJ, Kang SH, Suh SJ, Kim JH, Seo YS, *et al*: An explorative analysis for the role of serum miR-10b-3p levels in predicting response to sorafenib in patients with advanced hepatocellular carcinoma. J Korean Med Sci 32: 212-220, 2017.
42. Wang Y, Zhang X, Zhao Z and Xu H: Preliminary analysis of microRNAs expression profiling in MC3T3-E1 cells exposed to fluoride. Biol Trace Elem Res 176: 367-373, 2017.
43. Haimanot RT: Neurological complications of endemic skeletal fluorosis, with special emphasis on radiculo-myelopathy. Paraplegia 28: 244-251, 1990.
44. Liu L, Chen Y, Qi J, Zhang Y, He Y, Ni W, Li W, Zhang S, Sun S, Taketo MM, *et al*: Wnt activation protects against neomycin-induced hair cell damage in the mouse cochlea. Cell Death Dis 7: e2136, 2016.
45. Xia MY, Zhao XY, Huang QL, Sun HY, Sun C, Yuan J, He C, Sun Y, Huang X, Kong W, *et al*: Activation of Wnt/β-catenin signaling by lithium chloride attenuates d-galactose-induced neurodegeneration in the auditory cortex of a rat model of aging. FEBS Open Bio 7: 759-776, 2017.
46. Ni W, Zeng S, Li W, Chen Y, Zhang S, Tang M, Sun S, Chai R and Li H: Wnt activation followed by Notch inhibition promotes mitotic hair cell regeneration in the postnatal mouse cochlea. Oncotarget 7: 66754-66768, 2016.
47. Brennan E, Wang B, McClelland A, Mohan M, Marai M, Beuscart O, Derouiche S, Gray S, Pickering R, Tikellis C, *et al*: Protective effect of let-7 miRNA family in regulating inflammation in diabetes-associated atherosclerosis. Diabetes 66: 2266-2277, 2017.
48. Kumar M, Ahmad T, Sharma A, Mabalirajan U, Kulshreshtha A, Agrawal A and Ghosh B: Let-7 microRNA-mediated regulation of IL-13 and allergic airway inflammation. J Allergy Clin Immunol 128: 1077-85.e1, 10, 2011.
49. Block H, Ley K and Zarbock A: Severe impairment of leukocyte recruitment in ppGalNAcT-1-deficient mice. J Immunol 188: 5674-5681, 2012.